ELECTRONIC SUPPLEMENTARY INFORMATION

for

Protein-assisted 2D assembly of gold nanoparticles on a polysaccharide surface

by

Laura Taajamaa, Orlando J. Rojas, Janne Laine, Kirsi Yliniemi, Eero Kontturi

Contents

- Detailed description of the experimental work (Chapter Experimental details)
- Chart on chemical conversion of trimethylsilyl cellulose (TMSC) to cellulose (Fig. S1)
- Quartz-Crystal Microbalance with Dissipation monitoring (QCM-D) dissipation data (Fig. S2)
- QCM-D modelling results (Table S1)
- 2D atomic force microscopy (AFM) images of the PS/cellulose surfaces before and after gold nanoparticle (AuNP) assembly and individual height profiles extracted from the AFM height images of the modified blend films (Fig. S3)
- 2D AFM height images of PS/cellulose blend films before and after BSA assembly (Fig. S4)
- Assembly of cationic AuNPs in QCM-D (Fig. S5), AFM height images of PS films after the assembly (Fig. S6) and results from the QCM-D modelling and AFM image analysis from the PS films after assembly (Table S2)
- X-ray photoelectron spectroscopy (XPS) results (Table S3).

Experimental details

Materials

Trimethylsilyl cellulose (TMSC) (Fig. S1) was synthesized and characterized as described previously.[1, 2] Weight average molecular weight and number average molecular weight obtained from size-exclusion chromatography measurements were *ca.* 227000 and 79000 g/mol, respectively, and polydispersity index (PDI) was 2.9. The degree of substitution based on XPS results was 2.1. Polystyrene (PS) (Aldrich 182427) had molecular weight of 280 000 Da according to the manufacturer.

Albumin from bovine serum (BSA) was commercial product from Sigma-Aldrich (A7030). According to the manufacturer, purity was ≥98 %, the product was essentially fatty acid and globulin free and molecular weight was *ca.* 66 kDa. Gold nanoparticles (AuNPs) were purchased from Sigma-Aldrich (741965). The diameter was 20 nm, PDI<0.2, core size 18-22 nm and mean hydrodynamic diameter 28-36 nm, according to the manufacturer. Poly(allylamine hydrochloride) (PAH, Mw≈58 000, Aldrich) was used for depositing a cationic layer on commercial, anionic

AuNPs. HCl (Aldrich) was used to control the pH of the solution prior to the zetapotential measurements, if necessary.

All solvents and other chemicals were of analytical grade and used as obtained from the manufacturer. Water used was of ultra-high quality (UHQ) (resistivity 18.2 MΩ cm) purified with Millipore Direct-Q® 3UV (Millipore, Molsheim, France).

Methods

Spin Coating. Ultrathin films of PS and TMSC blends (here referred as PS/TMSC surfaces) were prepared by spin coating. TMSC and PS were separately dissolved in toluene with solution concentration of 10 g/dm^3. Blends were prepared by mixing the two 10 g/dm^3 solutions and diluting the rest with toluene in a way that the majority component concentration was always 5 g/dm^3 and the minority component concentration varied according to the PS/TMSC ratio. Pure cellulose and PS films were prepared from 5 g/l solution to obtain the same amount of polymer as in the blends. The spin coater used was WS-650SX-6NPP/LITE (Laurell Technologies Corporation, North Wales, PA, USA). AT-cut silicon dioxide QCM-D crystals (BiolinScientific, Västra Frölunda, Sweden) were used as substrates. Before mounting the substrates on the spin coater, they were cleaned in the UV/ozonator for at least 20 minutes and prior to spin coating the bare crystals were rinsed twice with toluene (4000 rpm for *ca.* 10 s). Spin coating was performed with the spinning speed of 4000 rpm and with the acceleration speed of 2130 rpm/s. The deposition of the solution was performed on a static substrate and the spinning was retained ca. 30 seconds after the disappearance of the Newtonian rings which usually took place already during the acceleration.

Selective conversion of TMSC to cellulose. The spin coated films containing TMSC (PS/TMSC surfaces) were hydrolysed in a 2 M aqueous HCl vapor environment under vacuum for 2 minutes to obtain PS/cellulose films. During the hydrolysis, TMSC is converted back to cellulose thus the TMSC patches contract due to the replacement of the bulky trimethylsilyl groups with tightly packed hydroxyl groups (Fig. S1).

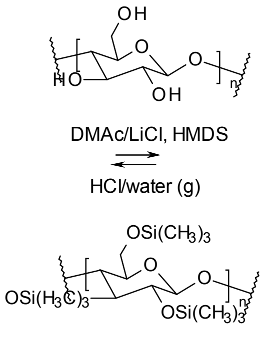

Fig. S1. Selective conversion of TMSC (bottom) to cellulose (top).

Preparation of cationic nanoparticles (AuNP-PAHs). Cationic AuNPs were synthesized by attaching electrostatically a cationic PAH layer on the top of the protective anionic layer of commercial AuNPs (*i.e.*, utilizing layer-by-layer method). 4 ml of anionic AuNPs were shaken with 4 ml of 2 mg/ml PAH solution for 20 min. The formed AuNP-PAHs were centrifuged to remove the excess of PAH solution, washed with water, centrifuged again and then re-dispersed into 1 ml of water.

Zetapotential measurements of AuNP-PAHs. Zetapotential measurements were performed with dynamic light scattering instrument (Zetasizer Nano series, Malvern Instruments Ltd) at 25°C, using a disposable zetapotential cell (folded capillary cells, Malvern Instruments Ltd). Data was analysed by the Zetasizer software (Malvern Instruments Ltd.) and using literature values of bulk Au for the refractive index and absorption at 633 nm (n=0.180, a=0.120).[3,4] The zetapotential of commercial, anionic AuNPs was measured prior to mixing with PAH solution and it was -20 mV (pH=6.5). Subsequently, to prove the formation of cationic AuNPs after AuNP-PAH synthesis, the zetapotential of Au-PAHs was measured and it was +39 mV (pH = 8.9). As PAH is a weak polyelectrolyte and its degree of ionization strongly depends on pH, the cationic nature of AuNP-PAHs was ensured also in the measurement conditions by determining zetapotential of AuNP-PAHs at pH = 7.5 and it was +22 mV.

AuNP assembly on polysaccharide surfaces using Quarts-Crystal Microbalance with Dissipation monitoring (QCM-D). Protein-assisted AuNP assembly was performed with a Q-Sense E4 instrument (Q-Sense AB, Gothenburg, Sweden). The crystals with PS/cellulose surfaces were immersed overnight in water and thoroughly dried with nitrogen gas. After the crystals had been mounted to the measuring chamber in QCM-D instrument, a continuous flow of dilute (≤0.01 μM) ammonium hydroxide solution was introduced to the chamber. The pH of ammonium hydroxide was adjusted close to eight. When a stable baseline was reached, the measurement was started and after ten minutes, BSA dissolved in dilute (≤0.01 μM) ammonium hydroxide solution was presented into the chamber. The pH of the 0.1 g/dm^3 BSA solution was the same as that of the pure dilute ammonium hydroxide. The isoelectric point (pI) of BSA is *ca.* at pH 5 thus during adsorption, it carries a negative net charge. Also cellulose surface has weak negative charge.[5] The BSA adsorption continued for 45 minutes and it was followed by a rinsing step with ammonium hydroxide and sodium acetate-acetic acid (NaAc/HAc) buffer (pH ~4.5) to remove any unbound BSA and to adjust BSA charge from anionic to cationic. Electrostatic attachment of citrate-stabilized AuNPs carrying negative charge into BSA patches was achieved by adjusting pH from *ca.* 8 to 4.5 with NaAc/HAc buffer. After the protein adsorption and rinsing steps, the 3.4 ng/dm^3 AuNP solution in NaAc/HAc buffer (pH ~4.5) was introduced and adsorption was continued for 30 minutes. In the case of cationic nanoparticles (AuNP-PAH), the pH during the adsorption was adjusted to 7.5 in order to retain BSA anionic. The surfaces were then rinsed with NaAc/HAc buffer (in the case of the anionic AuNPs only) and UHQ water (in the case of both anionic and cationic AuNPs) to remove any excess AuNPs. After the stabilization of the frequency and dissipation curves, the measurement was stopped. All measurements were recorded at 5 MHz fundamental resonance frequency and its overtones 15, 25, 35, 55 and 65 MHz and with constant 0.1 ml/min pump flow rate. Only the fifth overtone (25 MHz) is displayed in figures for clarity. The temperature was stabilized to 23ºC and each experiment was repeated at least two times. The QCM-D results were analysed quantitatively with Voigt model explained in more detail below.

Atomic Force Microscopy (AFM). Surface morphology was characterised using MultiMode 8 scanning probe microscope (Bruker AXS Inc., Madison, WI, USA). The images were scanned in tapping mode with E scanner and silicon cantilevers (NSC15/AIBS from Ultrasharp μmasch, Tallinn, Estonia). The radius of curvature for the tip according the manufacturer was less than 10 nm and typical resonance frequency of the cantilever was 325 kHz. At least two parallel surfaces were prepared and at least two points on each were imaged. No image processing besides flattening was performed. All quantitative data was extracted from the height images.

Image Analysis was performed using Nanoscope Analysis (version 1.20, Veeco, Plainview, NY, USA) and Scanning Probe Image Processor (SPIP) (version 6.0.2, Image Metrology, Lyngby, Denmark) softwares. The surface coverage of AuNPs was determined from $5 \times 5\ \mu m^2$ height images using the Particle and Pore analysis module in SPIP with Threshold algorithm. The Z-scale height parameter in 3D AFM images (Fig. 3) was adjusted to 50 nm and aspect ratio to 8.

X-Ray Photoelectron Spectroscopy (XPS). Chemistry of the surfaces was studied with XPS. XPS measurements were performed with an AXIS 165 (Kratos Analytical, Manchester, UK) spectrometer using a monochromated Al Kα X-ray source. All samples were pre-evacuated overnight to stabilize ultra-high vacuum (UHV) conditions. UHV condition was monitored during the whole measurement. Two parallel samples were prepared and each sample was analysed at three points. Elemental surface composition was determined from low resolution scans recorded with 80 eV pass energy and 1 eV steps. Relative amounts of nitrogen and gold were obtained from N 1s and Au 4f regional scans recorded with the same resolution and step intervals as survey scans, only with extended acquisition times. Carbon 1s and oxygen 1s high resolution spectra were determined using 20 eV pass energy at 0.1 eV steps. The carbon 1s emission was resolved into various contributions corresponding to distinct chemical states of carbon according to literature.[6]

Size-exclusion chromatography (SEC). The molecular weight of TMSC was determined with SEC using chloroform with 2% triethylamine (TEA) as eluent. Elution speed was 1 mL/min through the following column system: PLgel precolumn and PLgel, 104, 105, 103, and 102 Å columns supplied by Polymer laboratories. Relative changes in molecular weight were determined with a Waters RI-detector (refractive index) against polystyrene standards at 35 °C.

Additional results

QCM-D Dissipation data. QCM-D provides information not only on the adsorbed amount but also on the viscoelastic properties of the adsorbed layer via dissipation monitoring. Dissipation data is obtained by stopping the driving voltage and recording the decaying amplitude of the crystal as a function of time. Rigid layers have low dissipation values while more viscoelastic layers exhibit higher values due to short damping times caused by greater frictional losses. The dissipation changes as a function of time are shown in Fig. S2. Only minor changes in dissipation indicate that the adsorbed BSA and AuNPs were rigidly bound and did not swell or bound water significantly. Also, no major differences between the PS/cellulose blend ratios were noted. This is understandable since all the films that have cellulose as a majority component (PS/TMSC 0:1, 1:50, 1:20 and 1:5) contain the same amount of cellulose (5 g/dm^3 in the initial spin coating solution) and cellulose is the component that swells and binds water in these ultrathin films.

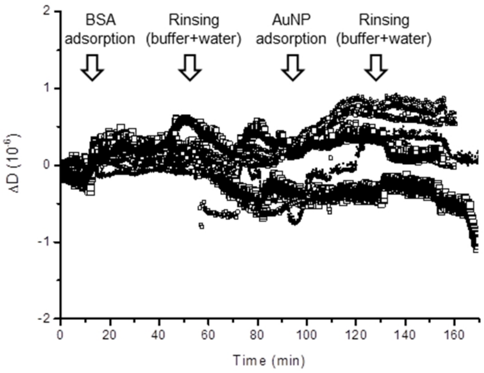

Fig. S2. AuNP assembly in QCM-D: changes in dissipation (ΔD) as a function of time. The label size increases with the increasing amount of PS in the film (from blend ratio PS/TMSC 0:1 to 1:0 films).

QCM-D Data Modelling. When the adsorbed component is evenly distributed and rigidly bound to the surface, and its mass low enough compared to the mass of the crystal, the adsorbed amount can be estimated with Sauerbrey's equation[7]

$$\Delta m = -\frac{C\Delta f}{n} \tag{S1}$$

where C is the mass sensitivity constant (C = 0.177 mg/(Hz $^{-1}$m^{-2}) for a 5 MHz crystal), n is the overtone number (n = 1, 3, 5...), and Δf is the observed change in frequency. If, however, the adsorbed layer does not meet the Sauerbrey conditions, the equation 1 underestimates the adsorbed mass. Voigt viscoelastic, parallel spring and damper iterative model was used to estimate the adsorbed masses of BSA and AuNPs on PS/cellulose blend surfaces. The calculations were performed with Q-Tools (version 2.1, Q-Sense, Västra Frölunda, Sweden) software. When the Voigt model is applied, certain assumptions need to be made and here 1200 g/m^3 was used for the density of the adsorbed layer.[8] The obtained values for the adsorbed BSA and AuNP masses (mg/m^2) are presented in Table S1.

Table S1. Results from the QCM-D modelling with Voigt model. The PS/TMSC blend ratios (w/w) from initial spin coating solutions are stated and blend ratios 0:1 and 1:0 correspond to cellulose and PS, respectively.

	Voigt mass (mg/m^2)	
PS/TMSC blend ratio	**BSA adsorption**	**AuNP adsorption**
0:1	0.00	0.00
1:50	0.28	1.77
1:20	0.12	1.10
1:5	1.17	3.77
2:5	1.97	4.26
1:0	4.31	5.00

Surface morphology evaluation. The surface morphology of the PS/cellulose films was characterised with AFM before and after the AuNP assembly (Fig. S3). Pure cellulose stays mainly intact during the AuNP assembly while PS film undergoes pronounced changes. BSA adsorbs selectively to PS domains in the blend films under these conditions. No major changes in the overall morphology of the blend films on a large scale were noted but once smaller scan sizes or individual height scans were observed the appearance of AuNP (diameter *ca.* 20 nm) was obvious. The citrate-stabilised particles seemed to stay stable also during adsorption since no major aggregates were noted in AFM images after the AuNP assembly. Also films at intermediate stage of the process (after BSA adsorption and rinsing step) were imaged but BSA seems to adsorb in such a flat conformation that no changes in the morphology were observed, even at high magnifications (Fig. S4).

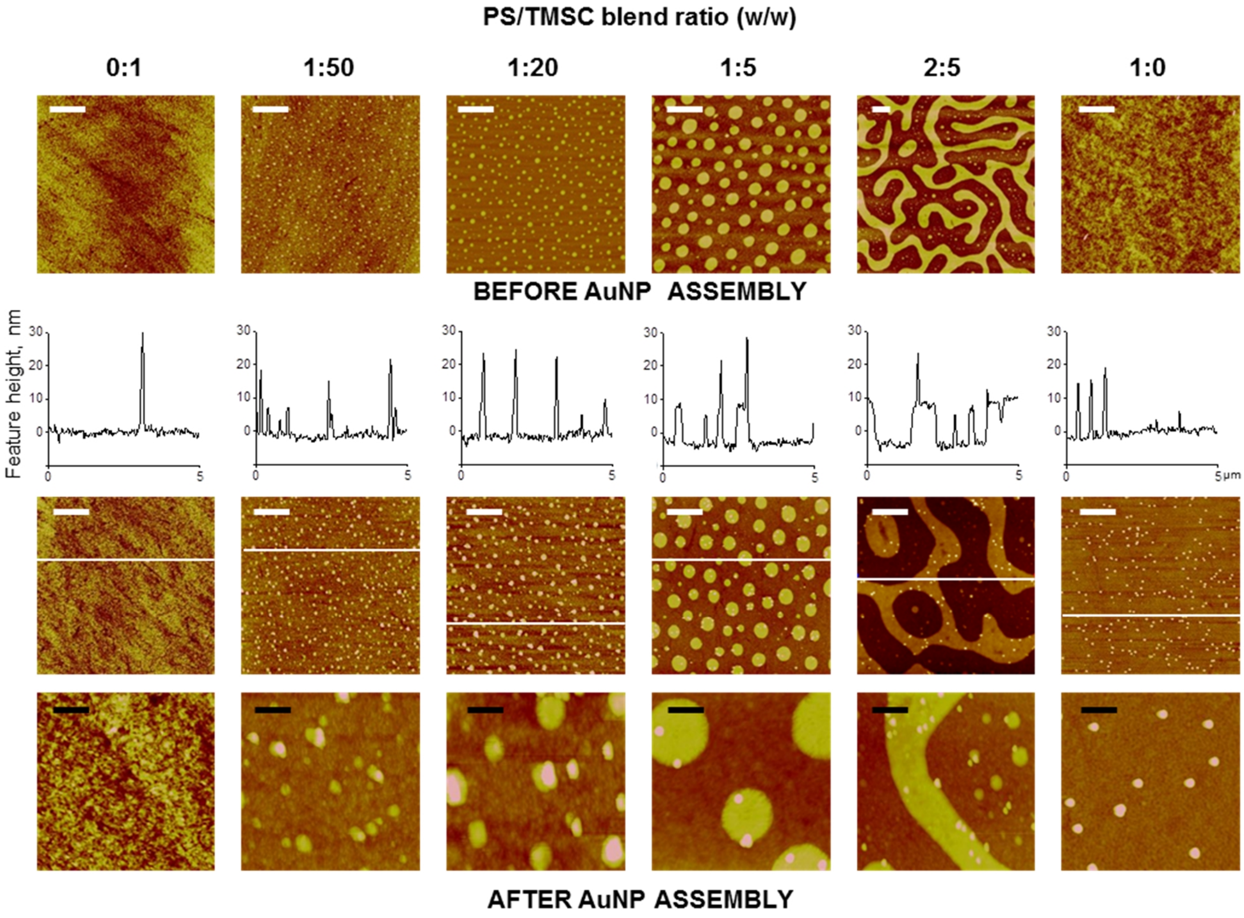

Fig. S3. Representative 2D AFM height images before (top row) and after (two bottom rows) AuNP assembly. White and black scale bar correspond to 1 µm and 200 nm, respectively. PS/TMSC blend ratios (w/w) in the initial spin coating solutions are stated on top. Blend ratio 0:1 and 1:0 correspond to cellulose and PS surfaces, respectively. In the AFM height images, the light areas are higher and dark areas are lower. On top of the 5 × 5µm^2 height images after the AuNP assembly, there are individual height scans and in the corresponding image, white line indicates the place where the height scan is taken. Note that horizontal scale accuracy is limited in AFM.

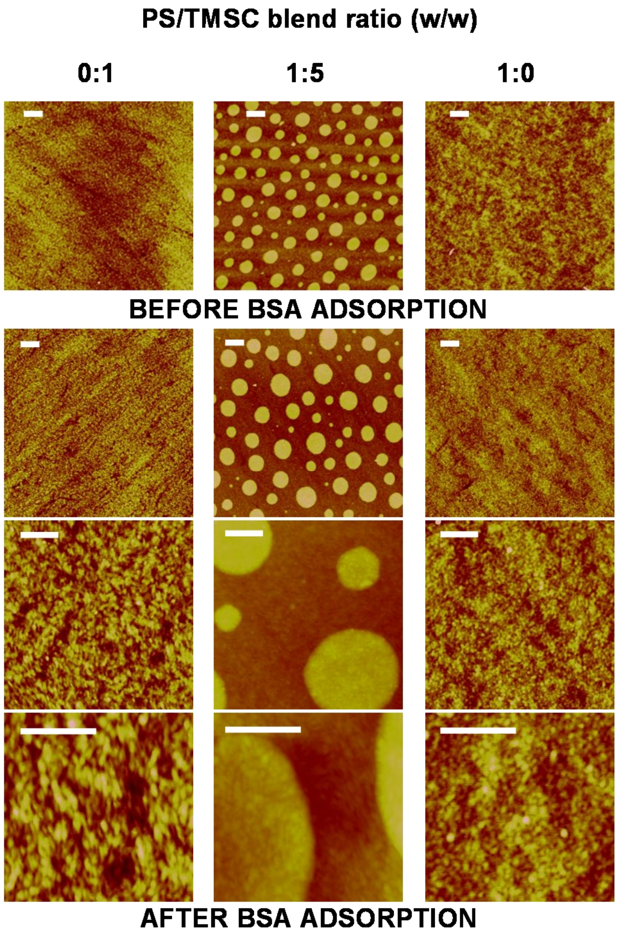

Fig. S4. Representative 2D AFM height images of PS/cellulose blend films before (top row) and after (three bottom rows) BSA assembly. The length of the scale bar is 200 nm in all images, i.e., the bottom three rows represent different magnifications. PS/TMSC blend ratios (w/w) in the initial spin coating solutions are stated on top. Blend ratio 0:1 and 1:0 correspond to cellulose and PS surfaces, respectively. In the AFM height images, the light areas are higher and dark areas are lower.

Adsorption of cationic AuNPs (AuNP-PAHs). BSA was adsorbed on a PS surface under similar adsorption conditions as described for the previous experiments. The adsorption was carried out for 20 minutes. Subsequently, the pH was tuned to 7.5 to retain the BSA anionic (isoelectric point at pH~5), and the surface was exposed to the AuNP-PAHs. Fig. S5 clearly shows that the procedure for attaching AuNP-PAHs on the BSA treated PS surface was successful: decrease in the frequency indicates an increased mass due to the adsorption of AuNP-PAHs.

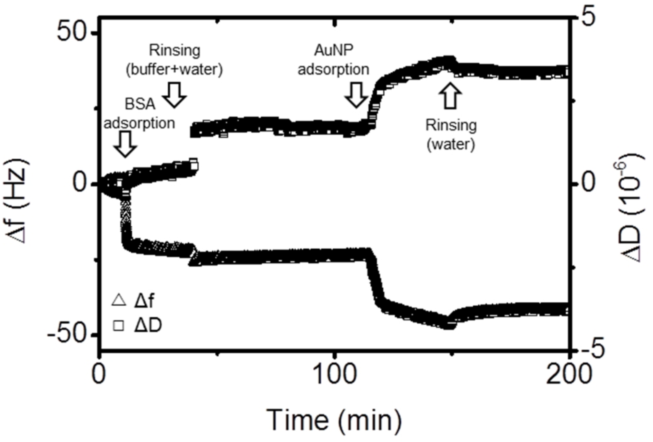

Fig. S5. The assembly of AuNP-PAHs in QCM-D: changes in frequency (Δf, △) and dissipation (ΔD, □) as a function of time.

The quantity of the adsorbed AuNP-PAHs was calculated from the QCM-D data of Fig. S5, according to the previously described Voigt modelling (see section QCM-D Data Modelling). Furthermore, the adsorbed amount of AuNP-PAHs was quantified by AFM imaging the surfaces and subjecting the images to image analysis as previously described. The AFM images are shown in Fig. S6, and Table S2 reveals the quantitative results from QCM-D and AFM analysis. It is evident that the amount of the adsorbed AuNP-PAHs is very similar to the values of the adsorbed anionic AuNPs (see Fig. 4 in the main article).

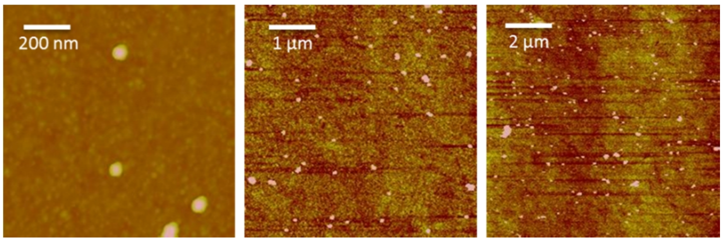

Fig. S6. AFM height images of PS films after sequential adsorption of BSA and AuNP-PAHs.

Table S2. Results from the QCM-D modelling with Voigt model and AFM image analysis from the PS films after sequential adsorption of BSA and AuNP-PAHs.

Blend ratio	AuNP-PAH Voigt mass, mg/m^2 (QCM)	Particle count (AFM)	Coverage, % (AFM)
PS/TMSC 1:0	5.50	188±18	1.7±0.18

Surface chemical composition. XPS was used to confirm the successful AuNP assembly on the PS/cellulose films (Table S2). The relative amounts of nitrogen (N 1s) and gold (Au 4f) emissions were used as fingerprints for BSA and AuNPs, respectively, since they are not present in the films before assembly. Generally, the more PS in the films, the higher the amount of both nitrogen and gold on the surface after AuNP assembly. However, in the case of PS/cellulose 2:5 the adsorbed amounts are smaller. This is hypothesized to derive from the fact that with this blend ratio the phase separation was more incomplete and also the domain sizes were larger. The phase separation occurs during rapid spin coating process and the TMSC (consequent cellulose) and PS phases contain traces of the other component as well. Also it has to be noted that the quantitative XPS analysis has its limitations and prerequisite is homogenous distribution of the components on the surface.

Table S3. XPS results. The PS/TMSC blend ratios (w/w) from initial spin coating solutions are stated and blend ratios 0:1 and 1:0 correspond to cellulose and PS, respectively.

	Atomic Concentrations					**C 1s Hi-Res components**			
Blend ratio	**O 1s**	**C 1s**	**Si 2p**	**N 1s**	**Au 4f**	**C-C**	**C-O**	**C=O**	**COC**
0:1	43.12±0.67	54.71±0.93	2.09±0.26	0.085±0.101	0±0	5.28	75.61	17.83	1.29
1:50	41.15±0.65	56.84±0.49	1.68±0.15	0.302±0.248	0.022±0.010	9.99	71.99	16.74	1.29
1:20	40.14±0.57	57.58±0.50	1.91±0.26	0.35±0.135	0.018±0.010	15.04	62.75	19.42	2.80
1:5	34.64±0.65	63.60±0.49	0.91±0.15	0.787±0.248	0.057±0.010	31.90	54.13	12.72	1.25
2:5	31.64±0.79	66.90±0.79	0.87±0.24	0.548±0.234	0.043±0.019	41.00	44.26	11.50	3.24
1:0	6.75±0.72	89.91±1.48	1.03±0.58	2.27±1.05	0.048±0.004	85.69	12.79	1.40	0.13

REFERENCES

1 E. Kontturi, P. C. Thuene and J. W. Niemantsverdriet, *Langmuir*, 2003, **19**, 5735.

2 E. Kontturi, M. Suchy, P. Penttila, B. Jean, K. Pirkkalainen, M. Torkkeli and R. Serimaa, *Biomacromolecules*, 2011, **12**, 770.

3 P. B. Johnson and R. W. Christy, *Physical Review B* 1972, **6**, 4370.

4 J. Doak, R. K. Gupta, K. Manivannan, K. Ghosh and P. K. Kahol, *Physica E* 2010, **42**, 1605.

5 M. Österberg, *J. Colloid Interface Sci.*, 2000, **229**, 620.

6 G. Beamson and D. Briggs, *High Resolution XPS of Organic Polymers*, John Wiley & Sons, Chichester, 1992.

7 Z. Sauerbrey, *Phys. C: Part. Fields*, 1959, **2**, 206.

8 M. V. Voinova, M. Rodahl, M. Jonson and B. Kasemo, *Phys. Scripta*, 1999, **59**, 391.